IJST, Transactions of Mechanical Engineering, Vol. 38, No. M1, pp 105-117
Printed in The Islamic Republic of Iran, 2014

CHARACTERISATION, TESTING AND SOFTWARE ANALYSIS OF AL-WC NANO COMPOSITES*

B. GNANASUNDARAJAYARAJA[1], ** N. SELVAKUMAR[2] AND R. MURUGESH[3]

[1, 2]Dept. of Mechanical Engineering, Mepco Schlenk Engineering College Sivakasi, Tamilnadu, India 626 005
Email: bgjeyaraja@yahoo.com
[3]Dept. of Mechanical Engineering, Sree Sowdambika College of Engineering, Aruppukottai, Tamilnadu, India

Abstract– In the present study, Al-WC (0, 5, 10, 15% weight fractions) nano composite was developed with WC particles as the reinforcement and Al particles as the base metal. The WC (99.5%, 20μm) is mixed (0,5,10 & 15% in weight fractions) with Al powder (99.5%, 60μm) and milled separately for 45 h using high energy ball mill (Pulversitte 6, Fritsch-Germany,50 WC balls,10mm,b/p 20:1,300 rpm). Characterisation (every 9 h) is done using SEM (Hitachi, and SU1510-Japan), Zetasizer (Malvern, Nano ZS90 - UK) and AFM (XE 70, Park Systems - Korea).The particles reach the nano size after 45 h of milling. The raw powders are compacted (200,250,300kN), sintered (450ºC) and furnace cooled (for 48 h) to prepare the specimens of various aspect ratios (0.3, 0.32, 0.36, 0.38, 0.4, 0.42). The Nano indentation (2nN, AFM, XE 70, Park Systems, Korea), non-destructive (Fallon Ultrasonics,100MHZ, FUI1050, Canada) and destructive testing (UTM,1MN,5mm/min,10 kN increments) are carried out on all preforms to evaluate mechanical (axial, hydrostatic, hoop stresses and strains), physical (density, acoustic impedance, hardness) and elastic (Young's, shear, bulk modulus and Poisson ratio) properties of the composites and then analysed (graphical analysis), and the composite having the best properties (Al-15WC, h/d 0.3,ρ_f 0.79) is identified. Then, its properties are fed into ANSYS Workbench software (Release14) and FEA analysis (Static structural,67500 nodes, Linear Solid185 type,38283 elements) is carried out on the piston (114.7mm³,1.83 kg), modelled using PRO-E software. The results show the substantial improvement of the properties of the Al-WC composites compared to the parent metal.

Keywords– Metal matrix composites, Al-WC composites, ultrasonic test, compressibility studies, SEM&EDX images, ANSYS analysis

1. INTRODUCTION

Advances in the fields of engineering and technology and rapid industrialisation demands completely newer materials. The Powder metallurgy and nano technology helps to meet this demand for newer materials by developing superior materials [1-4] required for specific applications. The nano composites have very good physical and mechanical properties than the parent materials as the individual particles retain their superior properties even after alloying. When the particle reaches the nano size [5-6], the bonding between the particles is very high when compared with the micron sized particles. Among the hard alloys and refractory carbides, WC finds a wide range of industrial applications, being used extensively in commercial applications such as tips for cutting and drilling tools, wear resistant parts in wire drawing, extrusion and carbide dies and wear-resistant surfaces in many types of machines [7].

In the present study, the authors have developed the aluminium based tungsten carbide nano composites for various proportions such as 5, 10, and 15% of WC (in weight) added with the base

*Received by the editors August 17, 2012; Accepted September 1, 2013.
**Corresponding author

aluminium metal through Mechanical Alloying Method. The characterisation is carried out using SEM&EDX, AFM images. Nano Indentation is carried out on the nano particles using the diamond nano indenter. The Atomic Force Microscope is used to record the whole process of nano indentation and the hardness of the nano particles is determined from which other mechanical properties are determined for the composite powder. The Non-destructive testing [8-9], compressibility studies [10] were carried (UTM, 1MN, 5mm/min, 10 kN increments) out on all preforms and the physical (density, acoustic impedance, hardness), elastic (young's, shear, bulk modulus and Poisson ratio) and mechanical (axial, hydrostatic, hoop stresses and strains) properties of the composites are found and compared and the best composite is identified. The properties of this best composite are fed into the ANSYS Workbench software (Release 14). FEA analysis was carried out on the piston[11] modelled using PRO-E software. All the results substantiate the enhancement of properties of Al-WC nano composites with the increase of reinforcement particles in the nano composites when compared to the parent aluminium.

2. MATERIALS AND METHODS

The WC (99.5%, 20μm) is mixed with aluminium powder (99.5%, 60μm) in proportions of 5%, 10% and 15% in weight in a glove box (M Braun, AB Star-Germany) under argon gas atmosphere. The mixers are milled separately for 45 hrs using Pulversitte 6 (Fritsch-Germany) high energy ball mill having 50 WC balls 10mm in diameter, ball to-powder weight ratio 20:1 and rotation speed of 300 rpm. The milled composite powder was mixed with acetone solution and treated in Ultrasonic sonicator (750W, 20 kHz, Sonics-USA) for about 30 minutes to separate particles from agglomeration after the completion of milling. The particle size is determined every 15 minutes using X-Ray Diffraction (XRD) Scanning Electron Microscopy (SEM, Hitachi, and SU1510-Japan), Zetasizer (Malvern, Nano ZS90 - UK) and AFM (XE 70, Park Systems - Korea). The complete characterisations of all these composites are done using these instruments. One sample of this characterisation is given in Fig. 1a-c where the SEM images of the nano composite are given.

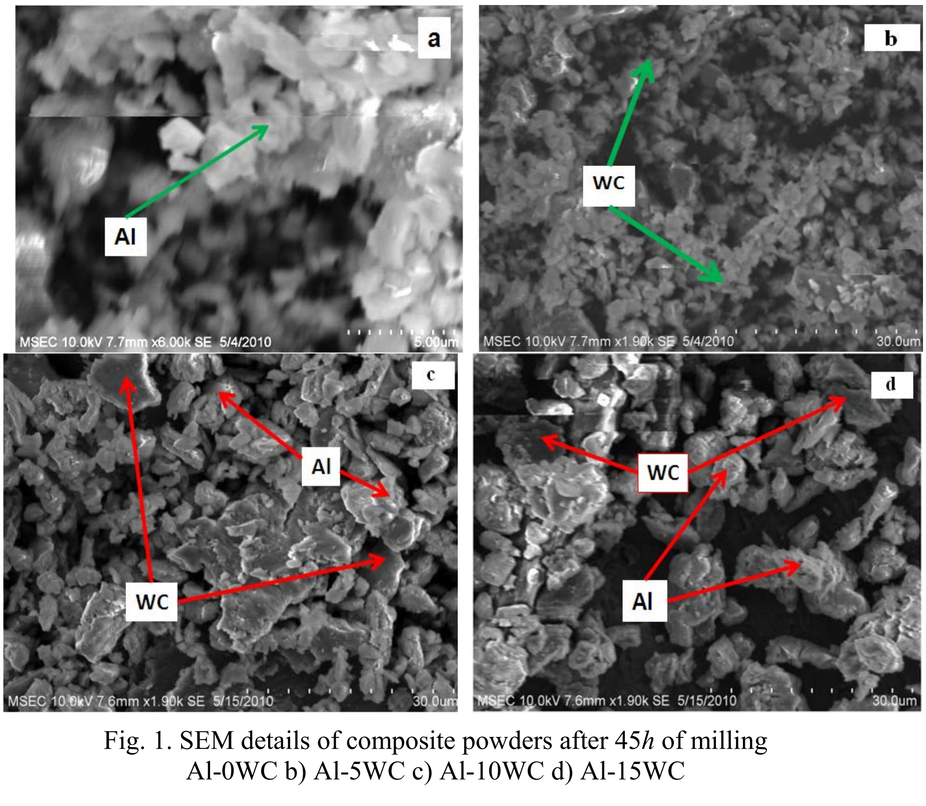

Fig. 1. SEM details of composite powders after 45*h* of milling
Al-0WC b) Al-5WC c) Al-10WC d) Al-15WC

The constant milling hour is used for all three compositions (5%, 10% and 15% of WC) of the nano composites. The particles reached the nano size after 45 hours of milling. From the AFM instruments the particle sizes of Al-0WC,Al-5WC, Al-10WC, Al-15WC are read as 6.388 nm, 59.99 nm,117.472 nm and 122.47 nm respectively. Using drop cast approach, a few drops of composite suspension prepared from sonicator are deposited on plain glass plate and allowed 10 minutes for drying and then nano indentation (Diamond Indenter) is carried out to identify the nano hardness. The powder mixtures are compacted for various loads to have various L/D ratios and sintered (450°C). The densities of the preforms are varied by varying compaction pressure (200kN, 250kN&300kN) and quantities of green powder are used. The non-destructive testing and compressibility studies were carried out on these specimens.

For non-destructive study, the ultrasonic velocity measurements have been carried out on all specimens using pulse echo method [8]. The NDT equipment consists of Ultrasonic receiver (Fallon Ultrasonic Inc. Ltd, FUI1050, Canada) with 100 MHz digital storage oscilloscope (Hewlett Packard-54600B) and X & Y cut PZT transducers (Frequency:10 MHz) for the generation and detection of longitudinal and shear Ultrasonic waves. The physical (density, acoustic impedance, hardness), elastic (young's, shear, bulk modulus and Poisson ratio) and mechanical (axial, hydrostatic, hoop stresses and strains) properties of the composites are found in this way and compared. From the tests, the best composite (Al-15WC, h/d 0.3, ρf 0.79) is identified and its properties are fed into ANSYS Workbench software (Release14) and FEA analysis (Static structural, 67500 nodes, Linear, Solid185 type, 38283 elements) is carried out on the piston (114.7mm^3, 1.83 kg) modelled using PRO-E software. All the results show the substantial improvement of the physical, elastic and mechanical properties of the Al-WC composites compared to the parent metal.

3. RESULTS AND DISCUSSIONS

a) Morphology using SEM

The samples were prepared for Scanning Electron Microscopy (SEM) investigation without ion sputter. Since it is a metal composite, ultrasonification is carried out for 0.25 *h* on the nano particles to prevent particles agglomeration. Then, a droplet of the composite is mixed with toluene and placed on the testing plate and SEM imaging is carried out. Different phases of the nano composites are distinguished by using Scanning Electron Microscopy (SEM, Hitachi, and SU1510-Japan). Figure 1a-d shows the SEM images of nano powder composites in which two different phases are identified.

- Figure 1a gives the images of Al-0WC powder in which aluminium particles appear like polished stones.
- Figure 1b provides the image of Al-5WC powder composite in which WC particles are deposited as black spots on the aluminium particles.
- Figure 1c shows the SEM image of Al-10WC composite powder in which the black spots on the aluminium granule show the deposition of WC on the aluminium matrix. Both spherical and flake-like structures are observed in the photograph.
- Figure 1d shows the SEM image of Al-15WC composite in which the WC particles are deposited as the black spots on the white aluminium flakes. Increasing percentage of WC increases the particle sizes of composites. This is because of the constant milling time (45hr) used for all composites and hard nature of secondary matrix (WC) compared to primary matrix (Al).

b) Topography using AFM

An AFM image of Al-0 to 15 WC composite is shown in Figure 2a-d. Particle distribution found in the 10X10 μm area is explored by a line scan carried out across the 2D image at 5μm and is represented as red line. Vertical line scan carried out at 6.5μm is indicated by the green line.

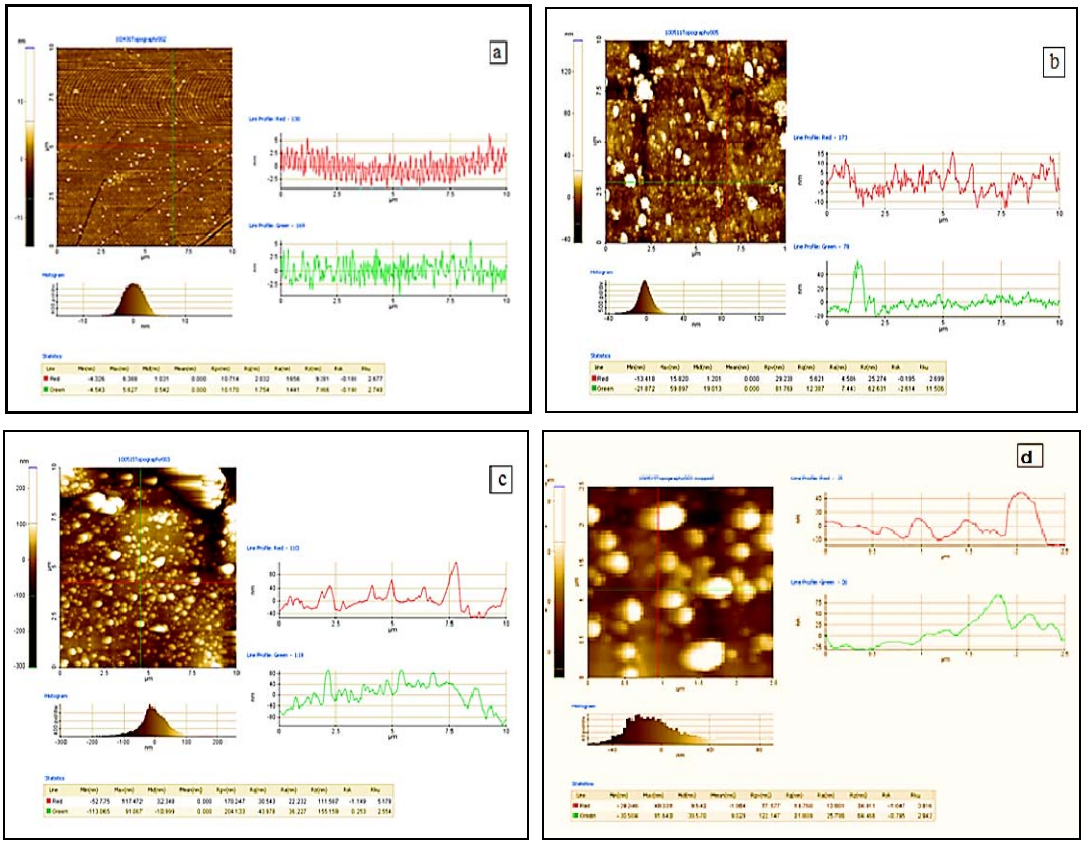

Fig. 2. AFM topography of composites after 45 *h* of milling
(a)Al-0WC b) Al-5WC b) Al-10WC d) Al-15WC

- In Fig. 2a, the maximum particle size and surface roughness (R_a) found on red line is 6.388 *nm*& 1.656 *nm* respectively. Along the green line it has maximum particle size and surface roughness (R_a) of 4.543 *nm* & 1.441 *nm* respectively.
- Similarly, Fig. 2b shows the topography of Al-5WC composite. The maximum particle size and surface roughness is approximately 59.99 *nm* and 7.443 *nm* respectively.
- Further, Fig. 2c represents the AFM image of Al-10WC powder. It is observed that the particles are distributed to the maximum size of 117.472 *nm* and surface roughness of the particles exist to the maximum size of 36.227 *nm*.
- Figure 2d represents the AFM image of Al-15WC powder. It is observed that the particles are distributed to the maximum size of 122.147 *nm* and surface roughness of the particles exist to the maximum size of 25.786 *nm.*
- It is further deduced from Fig. 2a-d that, when the WC content increases, particles are coarser and their sizes and roughness values increase. This is because the particle size reduction takes more time with the increase of WC content in primary matrix, but in the experiment, constant milling time of 45*h* is maintained for all three composites for comparison purposes. Hence particles are coarser with the increase of hard secondary matrix (WC) in the soft primary matrix (Al).

c) Nano indentation

Nano indentation is a new method to characterize mechanical and physical properties of the material on a very small scale. Nano indentation is performed in conjunction with AFM imaging. The complete nano indentation test can be visualised by AFM imaging. The data like indentations area, depth of penetration and force variations in test can be had from AFM image. In this study, the Al-WC (0, 5, 10, and 15) composite powder sample is prepared individually and placed on the sample holder of the SPM (Scanning Probe Microscope) instrument. The nano diamond tip is pressed into the sample and held for 1minute inside the sample and then it is removed. The maximum force of 2nN is applied and the depth of penetration is noted using F/D curve as shown in Fig. 3a-d. The experiment is conducted in this way for all the nano composite powder consistsing of 0,5, 10, 15% (in weight) of WC with the primary matrix of aluminium powder and the F/D curve is obtained.

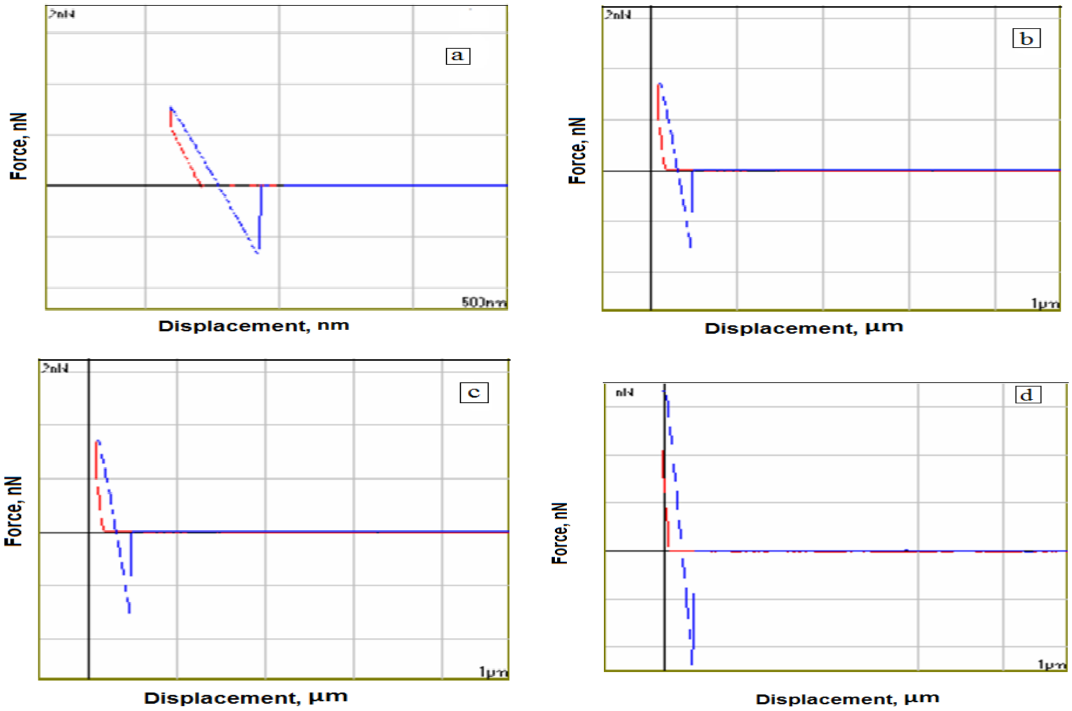

Fig. 3. F/D curves for composites
(a).Al-0WC (b) Al-5WC (c) Al-10WC and (d) Al-15WC

From the F/D curve, the following inferences are obtained.

- Initially, when the indentation progresses, the force required for indentation increases which is indicated by the first line in the F/D curve.
- After applying the denoted highest load (2nN), the tip freely penetrates the material which is shown by the inclined (dotted) second line following the first line in the F/D curve.
- Then, the tip is removed gradually from the material. At this time, again the metal slightly resists the movement of nano indenter depending on material property. Hence the force slightly increases when the indenter is removed which is indicated by the third line following the inclined second line.
- Next, the tip gradually comes out and the force required gradually decreases, which is shown in the fourth vertical line.
- From Fig. 3 (a-d),it is observed that the force of indentation increases with the increase of WC content. This is because of the increase in strength of the nano composites with the increase of WC content in the composite. The composite powder sample has a different deformation (h_c)

value for the load input of 2nN in proportion to the percentage (in weight) of reinforcement material (WC) added in the primary matrix of aluminium powder.

- The (h_c) value is calculated on the average value of the result of the experiment conducted by selecting four different points in the same sample of a selected composition of WC and Al metal matrix composite. The (h_c) value is calculated in this way for every composition (0,5, 10, 15% in weight) of WC with aluminium powder.
- From the results, it is shown that the penetration depth value (h_c) decreases with the increase of WC content present in the Al-WC metal matrix composite. This is because of the increase in strength of the composite in proportion to the increase in value of WC contents in the composites.
- The hardness (H) value can be calculated by using the formula (1):

$$H = \frac{P}{24.5(h_c)^2} \tag{1}$$

where P- Maximum applied load: h_c- Penetration depth.

- It is deduced from Table 1 that, increasing Wt. % of WC increases hardness which substantiates the SEM results obtained.

Table 1. Nano hardness of various composites

S. No	Composite	*P,nN*	*h_c,nm*	*H,MPa*
1.	Al-0WC	2.0	546	273
2.	Al-5WC	2.0	489	341
3.	Al-10WC	2.0	382	559
4.	Al-15WC	2.0	348	674

d) Ultrasonic testing

In this study, the ultrasonic velocity measurements have been carried out on all specimens using pulse echo method [8]. The NDT equipment consists of Ultrasonic receiver (Fallon Ultrasonic Inc. Ltd, FUI1050, Canada) with 100 MHz digital storage oscilloscope (Hewlett Packard-54600B) and X & Y cut PZT transducers (Frequency:10 MHz) for the generation and detection of longitudinal and shear Ultrasonic waves. An echo is registered each time the transmitted pulse is received by the same transducer. The echo travels a distance ‘2D’ in the specimen, where ‘D’ is the height of the preform. The time taken for the ultrasonic wave to travel through the specimen is noted from the CRO using cross correlation technique and from these values, the elastic and physical properties of the preform are calculated using the formula described in ref. [8] and tabulated in Table 2. The properties are then compared with aluminium preform to identify the contribution of WC in improving strength of the composites. The instrument has separate *X* and *Y* cut probes to measure the time taken for the ultrasonic waves in longitudinal (*X*) and shear plane (*Y*) directions respectively. From these values, other properties are calculated as described below. The ultrasonic longitudinal velocity (U_L) is calculated using Eqn. (2) (Rajendran et al 2003):

$$U_L = \frac{2h}{t_L} \tag{2}$$

where *h* is the height of the preform and ‘t_L’ is the time taken for the pulse wave to pass through the preform in longitudinal direction in μs which is found using *X* cut probe of the instrument. Next, velocity in *Y* direction through shear plane is calculated using Eq. (3).

$$U_s = \frac{2h}{t_s} \tag{3}$$

where,'t_S' is the time taken for the pulse wave to pass through the preform in Y direction in μs found using Y cut probe of the instrument.

Table 2. Various properties of composites calculated using ultrasonic testing

Composites	h, mm	D, mm	h/D,	ρ, kg/m^3	$\rho_f=\rho/\rho_{TH}$	Δt_L, μs	Δt_S, μs	U_L, m/s	U_S, m/s	E, GPa	G, GPa	K, GPa	μ	Z, MPa.s/m	H, MPa
Al-0WC	8.38	19.95	0.42	2510	0.93	3.40	5.57	4930	3010	60.88	22.72	63.42	0.34	12.35	242.31
	8.08	19.72	0.41	2550	0.94	3.24	5.30	4990	3050	63.53	23.71	66.18	0.34	12.72	252.86
	8.02	20.04	0.40	2560	0.95	3.20	5.24	5010	3060	64.23	23.97	66.91	0.34	12.82	255.64
	7.93	20.34	0.39	2570	0.95	3.16	5.17	5020	3070	64.71	24.15	67.41	0.34	12.89	257.55
	7.99	21.04	0.38	2580	0.96	3.16	5.17	5060	3090	66.12	24.67	68.88	0.34	13.06	263.16
	7.61	20.55	0.37	2590	0.96	3.00	4.91	5070	3100	66.61	24.85	69.39	0.34	13.13	265.11
Al-5WC	7.82	20.04	0.39	2920	0.87	3.00	4.89	5210	3200	79.31	29.82	77.75	0.33	15.21	337.91
	7.72	20.32	0.38	2930	0.88	2.92	4.76	5290	3250	82.13	30.88	80.52	0.33	15.51	349.93
	7.77	20.99	0.37	2940	0.88	2.92	4.76	5320	3260	83.13	31.25	81.50	0.33	15.63	354.19
	7.65	21.24	0.36	2950	0.88	2.88	4.70	5310	3260	83.17	31.27	81.54	0.33	15.67	354.36
	7.65	21.85	0.35	2960	0.88	2.88	4.70	5310	3250	83.31	31.32	81.68	0.33	15.70	354.95
	7.55	22.21	0.34	3000	0.90	2.86	4.67	5280	3230	83.51	31.39	81.87	0.33	15.83	355.81
Al-10WC	7.48	20.21	0.37	3150	0.79	2.80	4.56	5340	3280	89.60	33.94	82.96	0.32	16.79	407.27
	7.32	20.32	0.36	3180	0.80	2.75	4.47	5320	3270	89.87	34.04	83.21	0.32	16.91	408.50
	7.32	20.91	0.35	3190	0.80	2.72	4.42	5380	3310	92.36	34.98	85.52	0.32	17.16	419.82
	7.22	21.24	0.34	3200	0.80	2.68	4.35	5390	3320	93.09	35.26	86.19	0.32	17.26	423.14
	7.24	21.93	0.33	3250	0.81	2.68	4.35	5400	3330	94.90	35.95	87.87	0.32	17.56	431.36
	7.15	22.33	0.32	3280	0.82	2.65	4.31	5390	3320	95.40	36.14	88.33	0.32	17.69	433.64
Al-15WC	7.01	20.03	0.35	3610	0.78	2.65	4.29	5290	3270	100.96	38.53	88.56	0.31	19.09	488.10
	6.80	19.99	0.34	3620	0.78	2.56	4.15	5310	3280	102.00	38.93	89.47	0.31	19.22	493.11
	6.31	19.13	0.33	3630	0.78	2.36	3.82	5350	3300	103.84	39.63	91.09	0.31	19.41	502.03
	6.24	19.50	0.32	3640	0.79	2.32	3.76	5380	3320	105.21	40.16	92.29	0.31	19.57	508.65
	6.31	20.36	0.31	3650	0.79	2.32	3.76	5440	3360	107.89	41.18	94.64	0.31	19.84	521.61
	6.22	20.75	0.30	3660	0.79	2.28	3.69	5460	3380	109.26	41.7	95.84	0.31	20.00	528.23

Young's modulus
$$E = U_L \rho^2 \tag{4}$$

Shear modulus
$$G = U_s \rho^2 \tag{5}$$

where U_L and U_S is the ultrasonic velocity of wave in longitudinal and shear plane respectively. The density of the preform (ρ) is calculated using the Archimedes principle using Eqn. (6).

$$\rho = \frac{W_a \rho_w}{(W_a - W_w)} \tag{6}$$

Where W_a & W_w is the weight in air & water respectively and ρ_w is the density of water. Bulk modulus values of the nano composites can be calculated using the reference Rajendran et al 2006 and tabulated in Table 2.

Bulk modulus $$K = \frac{EG}{3(3G - E)} \tag{7}$$

Poisson Ratio $$\mu = \frac{E}{2G} - 1 \tag{8}$$

Micro hardness $$H = \frac{(1 - 2\mu)}{6(1 + \mu)} \tag{9}$$

Acoustical Impedance $$Z = U_L \rho \tag{10}$$

From the Table 2, it is deduced that

- The Young's, shear and bulk modulus values increase with the increase of WC contents in the composite because the material becomes stronger with the increase of WC contents in the composites causing lesser strain to the material.
- Similarly when the fractional density values increases the strength of the composite increases which strongly resists the deformations and failure of the material and hence
- Strains of the composite decrease. Because of this, Young's shear and bulk modulus values increase steadily for all the composites.
- Shear modulus describes the material's response to shearing strains (the deformation of shape at constant volume) when acted upon by opposing forces. These values are almost one third of the young's modulus values, which implies that the composite can withstand approximately 1/3 of the axial force when it is experiencing shear or twist force.
- Acoustic impedance is the property of the material which offers resistance to the sound waves passing through it. It is a proven fact that sound wave passes easily in a stronger medium than the lighter material. The higher the values of acoustic impedance, the higher the strength of the material. The values in Table 1 substantiate this property where the acoustic impedance values increase with the increase of WC content.
- The term "micro hardness" has been widely employed in the literature to describe the hardness testing of materials with low applied loads. The values in the table show the increase of hardness of the composite with the increase of WC contents and density of the composite.
- Thus increase of secondary particulate WC content increases the properties (young, shear, bulk modulus, hardness, acoustic impedance) of the composite in all aspects.

e) Compressibility testing

The preforms are prepared based on the procedure discussed in sec 2. The upsetting tests were conducted on an UTM having capacity of 1.0 *MN*, at room temperature using MOS_2 as the lubricant for all the specimens. The upsetting operation was carried out at the speed of 5*mm*/*min*. Initial diameter (D_0), the initial height (H_0) and the initial preform density (ρ_0) of the specimens were measured. Moreover, the density measurements of the preforms were carried out using the Archimedes principle. The weight of preform in air (W_a) and in water (W_w) was determined using digital balance and tabulated. Each compact was subjected to compressive loading in steps of 10 *kN* until the appearance of visible cracks on the free surface. Immediately after each incremental loading, the contact diameter at the top (D_{CT}), the contact diameter at the bottom (D_{CB}), the bulged diameter (D_B), the height of the preforms (H_f) and the density were recorded. Based on these data the various properties are calculated as discussed below. As explained by Narayanasamy et al. (2008), the different strains can be calculated as shown below:

Axial strain

$$\varepsilon_z = \ln\left(\frac{H_0}{H_f}\right) \tag{11}$$

Hoop strain

$$\varepsilon_\theta = \ln\left(\frac{\left[2D_B^2 + D_C^2\right]}{3D_O^2}\right) \tag{12}$$

where D_0 is the initial diameter of the preform before deformation
D_C is the contact diameter of the preform after deformation
D_B is the bulged diameter of the preform after deformation
H_0 is the initial height of the cylindrical preform before deformation and
H_f is the height of the barrelled cylinder after deformation

Conventional hoop strain

$$\varepsilon_\theta^{'} = \ln\left(\frac{D_c}{D_0}\right) \tag{13}$$

The Poisson's ratio

$$\nu = \frac{\varepsilon_\theta}{2\varepsilon_z} \tag{14}$$

Hoop stress

$$\sigma_\theta = \left(\frac{\alpha + \nu}{1 + \alpha\nu}\right)\sigma_z \tag{15}$$

where α is the slope between the hoop strain (ε_θ) and the axial strain (ε_z) and $\nu$is the Poisson's ratio, calculated based on $\varepsilon_\theta$and ε_z. Now substituting the value for the true axial stress the true hoop stress (σ_θ) can be calculated. The axial stress (σ_z) can be calculated [18] using the following expression

$$\sigma_z = \frac{\text{Load}}{\text{contact surface area}} \tag{16}$$

Further, using the values of the axial stress (σ_z) and the hoop stress (σ_θ), the hydrostatic stress (σ_m) can be calculated using the relationship given below:

$$\sigma_m = \frac{1}{3}\left(\sigma_\theta \approx \sigma_z\right) \tag{17}$$

Usually the axial stress (σ_z) is negative because it is compressive in nature. The upset forming test is conducted for all the preforms (24 preforms) and the properties are calculated using the above relations and are tabulated separately (24 separate tables).Then the properties are analysed graphically which is shown in Figs. 4 and 5 and is presented in detail in the following sections.

1. Hoop strain and axial strain:

- In the graphs 4(a-d), the maximum axial strain values represented in X axis decreases gradually with the increase of WC contents in the composites as 0.48, 0.40, 0.25 and 0.15. Similarly in the graphs 4 (a-d), the maximum hoop strain values marked in the Y axis also decrease as 0.48, 0.40, 0.35 and 0.20.

- This is because the strength of the composite increases with the increase of WC contents and hence, the deformation is less in both the axial and lateral directions of the composites. This decrease of deformation values gives fewer axial and hoop strain values for the composites with the increase of WC contents.
- Thus the Al-15WC composite made with the compaction load of 300 *kN* exhibits higher strength than other composites and parent aluminium metal. For this reason, this composite has a lower value of axial strain and hoop strain when compared to other composites. This is clearly visible in the graphs.

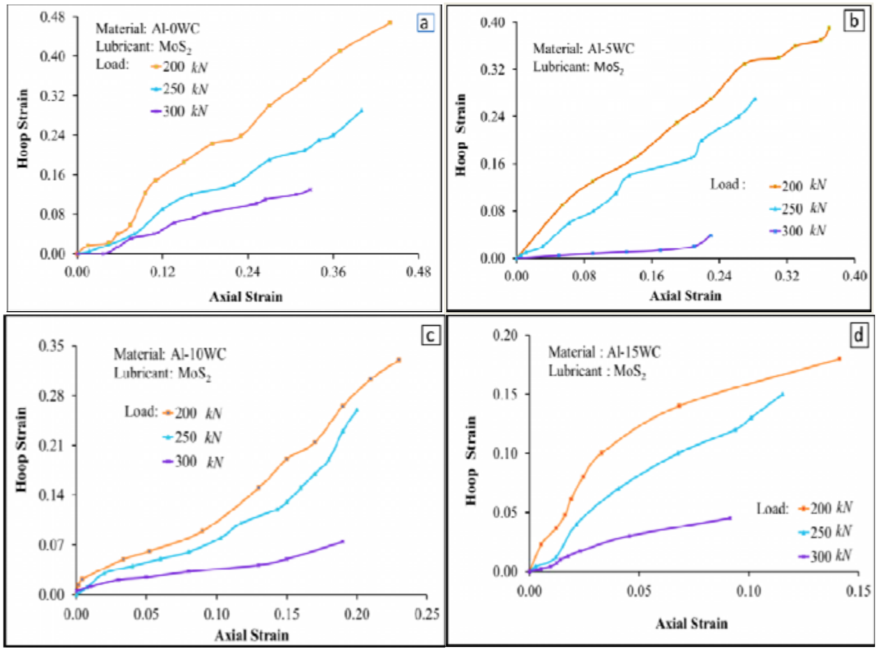

Fig. 4. Relation between hoop strain and axial strain of the composites
(a) Al-0WC (b) Al-5WC (c) Al-10WC and (d) Al-15WC

2. Various stresses and axial strain:

- In all the graphs shown in Figs. 5a-d, the axial and hoop stress values gradually increase with the increase of axial strain values.
- When the preforms are compressed uniformly in the axial direction, the preforms bulge proportionately in the lateral direction, hence the axial and hoop strain curves have a similar trend.
- Also, the axial strain values gradually decrease with the increase of WC contents. To cause the same axial strain values, say 0.1, the stress values required increase dramatically with the increase of WC contents in the composites. This implies that the strength of the composites increases with the increase of WC contents and hence it heavily resists the stresses acting on it and causes less deformation.
- In all the graphs, it is seen that the hydrostatic stress values are much less when compared to other stresses for all the composites. Hydrostatic stress is the volumetric mean stress acting uniformly throughout the entire specimen and is useful for the materials used in aerospace and marine applications where uniform fluid pressure will be acting on the material being used. This implies that the composite is so strong against the hydrostatic stresses acting on it.
- From all these graphs, it is evident that the composite Al-15WC has a higher strength than other composites.

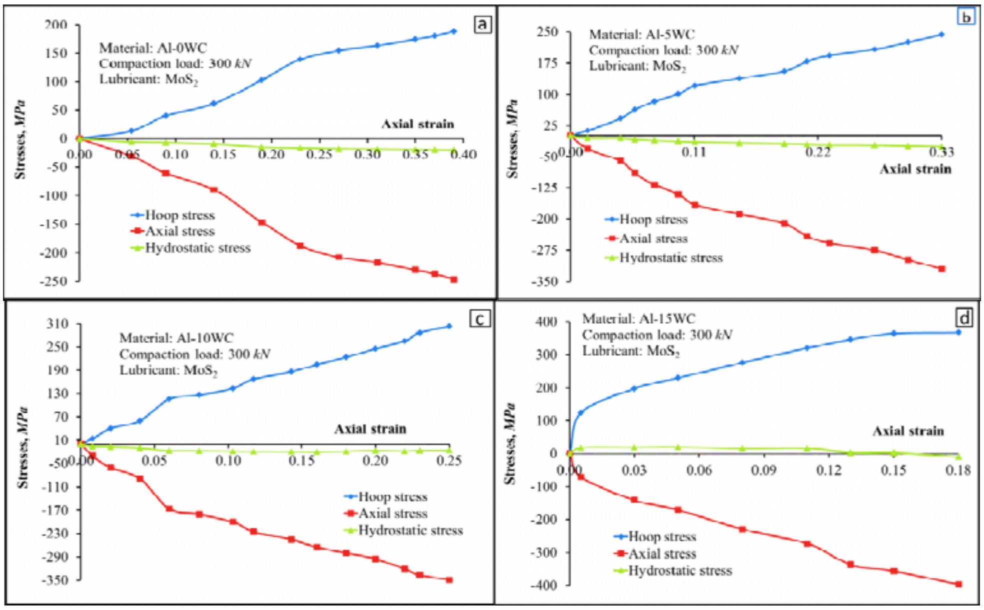

Fig. 5. Relation between various stresses for the composites
(a) Al-0WC (b) Al-5WC (c) Al-10WC and (d) Al-15WC

f) FEA analysis

- The FEA [14] analysis (Static structural,67500 nodes, Linear Solid185 type,38283 elements) using ANSYS Workbench software(Release 14) is carried out on a piston (114.7mm³,1.83 kg) made of Al-15%WC composite(h/d 0.3,ρf 0.79
- A load of 39kN [11] is applied on the top of the piston as the fuel pressure acts on the top of the piston and the piston is constrained at the bottom as the piston as the connecting rod is connected at the bottom end.
- The red colour in the component indicates the presence of higher value of max. Principal stress (1198.8 GPa), shear stress (1517 GPa), equivalent (Vonmises) stress (2855.7 GPa), and Normal stress (1099.3 GPa) values on the component (Table 3).
- The blue colour indicates the presence of lower values of principal stresses (0.703 MPa), shear stresses (0.141 MPa), equivalent stresses (0.263 MPa), and normal stresses (- 1835.9 GPa) acting on the component.
- The stress concentration is naturally more in the area where the material has grooves slots etc. Similarly, the stress concentrations are high in the area where the load is applied. This is shown in the figures.

Table 3. The maximum and minimum values of the mechanical properties

Sl. No	Mechanical parameters	Max. Value	Min. Value
1.	Normal Stress,GPa	1099.3	- 1835.9
2.	Equivalent (Von-Mises) Stress, GPa	2855.7	13.899
3.	Max.Principal stress value, GPa	1198.8	- 1481.0
4.	Maximum Shear stress, GPa	1517	7.7596

- In the software analysis shown in Fig. 6a-d, the areas of maximum stresses are shown in red, which appear in a lesser amount compared to the dark blue colour which corresponds to lower stress distributions. Especially in Fig. 6a&c, dark blue colour appears in larger amount which asserts the lower shear and Von mises stress distributions on the component.

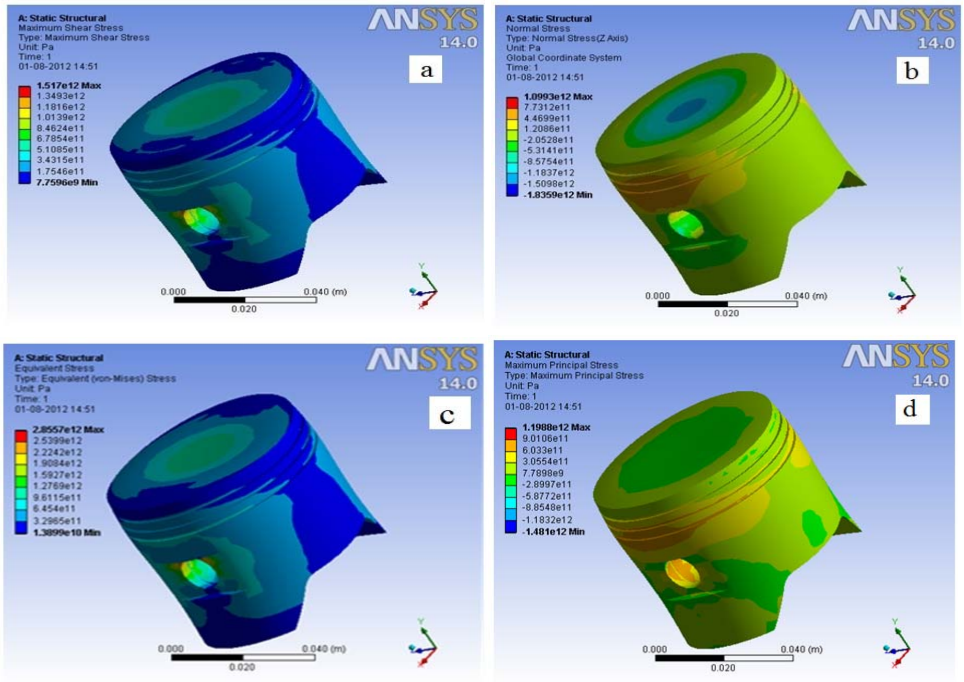

Fig. 6(a-d). FEA analysis of the Al-15WC composites

- This proves the increase in strength of Al-15%WC composites in practical applications substantiating previous results. As the strength of the composite is high, the stresses induced on the material are much less for the applied load of 39 kN, which is why the red colour which corresponds to maximum value of stresses appears in a lower amount compared to blue colour which corresponds to lower stresses induced on the material.

4. CONCLUSION

The conclusions that can be drawn from the test results are as follows.

- The Non-destructive test results show the substantial improvement of elastic properties of Al-WC composite compared to the parent metal aluminium.
- The upset forming studies shows that the Al-WC composite materials withstand the hydrostatic, hoop and axial stresses and axial strain well compared to the parent metal.
- The FEA analysis shows that the piston component possessing the properties of Al-WC composite has higher strength and withstands the principal, shear normal and Von mises stresses well and the deformation value which is the measure of failure of the material is also less for this composite material.
- All the studies show that the percentage of increase of WC contents increases the properties of the Al-WC composite proportionately.

REFERENCES

1. Najafi, A. & Eghtesad, M. (2013). Asymptotic stabilization of composite plates under fluid loading. *Iranian Journal of Science & Technology, Transactions of Mechanical Engineering*, Vol. 37, No.1, pp. 53-62.
2. Rabienataj Darzi, A. A., Farhadi, M. & Jourabian, M. (2013). Lattice Boltzmann simulation of heat transfer enhancement during melting by using nano particles. *Iranian Journal of Science & Technology, Transactions of Mechanical Engineering*, Vol. 37, No. 1, pp. 23-37.

3. Nabi, S. & Shirani, E. (2012). Simultaneous effects of brownian motion and clustering of nano particles on thermal conductivity of nano fluids. *Iranian Journal of Science & Technology, Transactions of Mechanical Engineering*, Vol. 36, No. 1, pp. 53-68.
4. Allahkaram, S. R. & Bigdeli, F. (2010). Influence of particle size on corrosion resistance of electroless Ni-P-Sic composite coatings. *Iranian Journal of Science & Technology, Transaction B: Engineering*, Vol. 34, No. 2, pp. 231-234.
5. Okumuş, F. (2004). An analysis of shear correction factors in a thermoplastic composite cantilever beam. *Iranian Journal of Science & Technology, Transaction B: Engineering*, Vol. 28, No 4, pp. 501-504.
6. Darvizeh, M., Darvizeh, A., Ansari, R. & Sharma, C. B. (2003). Buckling of fibrous composite cylindrical shells with non-condtant radius subjected to different types of Loading. *Iranian Journal of Science & Technology, Transaction B: Engineering*, Vol. 27, No 3, pp. 535-550.
7. Sherif El-Eskandarany, M. (2005). Fabrication and characterizations of new nanocomposite WC/Al_2O_3, materials by room temperature ball milling and subsequent consolidation. *J Alloys Compd*, Vol. 391, pp. 228–235.
8. Rajendran, V., Palanivelu, N., Chaudhuri, B. K. & Goswami, K. (2003). Characterisation of semiconducting V_2O_5–Bi_2O_3–TeO_2 glasses. *J Non-Cryst Solids*, Vol. 320, pp. 195-209.
9. Mahdavinejad, R. (2005). Finite element dimensional design and modeling of an ultrasonic transducer. *Iranian Journal of Science & Technology, Transaction B: Engineering*, Vol. 29, No. 2, pp. 253-263.
10. Narayanasamy, R., Ramesh, T. & Pandey, K. S. (2008). An experimental investigation on strain hardening behaviour of aluminium -3.5% alumina powder metallurgy composite preform under various stress states during cold upset forming. *Mater Des*, Vol. 29, No. 6, pp. 1212-1227.
11. Szurgott, P. & Niezgoda, T. (2011). Thermo mechanical FE Analysis of the engine piston made of composite material with low Histeresis. *J. KONES Power train and Transport*, Vol. 18, No. 1.